Coherent Effects of High-Energy Particles in a Graded $Si_{1-x}Ge_x$ Crystal

E. Bagli, L. Bandiera, V. Guidi,* and A. Mazzolari

INFN Sezione di Ferrara, Dipartimento di Fisica e Scienze della Terra, Università di Ferrara Via Saragat 1, 44100 Ferrara, Italy

D. De Salvador and G. Maggioni

*INFN Laboratori Nazionali di Legnaro, Viale dellUniversità 2, 35020 Legnaro, Italy and Dipartimento di Fisica,
Universitá di Padova, Via Marzolo 8, 35131 Padova, Italy*

A. Berra, D. Lietti, and M. Prest

*Università dell'Insubria, via Valleggio 11, 22100 Como, Italy and INFN Sezione di Milano Bicocca,
Piazza della Scienza 3, 20126 Milano, Italy*

E. Vallazza

INFN Sezione di Trieste, Via Valerio 2, 34127 Trieste, Italy

N. V. Abrosimov

Institute for Crystal Growth, 12489 Berlin, Germany

A graded $Si_{1-x}Ge_x$ crystal has been manufactured for operation with high-energy protons to excite coherent interactions of the particles with the crystal such as channeling and volume reflection. The crystal had the shape of a parallelepiped though its (111) atomic planes were curved at a radius of 25.6 m because of the graded Ge content. The crystal was exposed to a 400 GeV/c proton beam at the external lines of CERN Super Proton Synchrotron to probe its capability to steer high-energy particles. Measured deflection efficiency was 62.0% under planar channeling and 96.0% under volume reflection. Such values are critically compared to their counterparts for a standard bent Si crystal under peer conditions. A Monte Carlo simulation of the dynamics of channeled and volume reflected particles in a graded crystal including the effect of Ge impurities and of lattice dislocations has been carried out. We found that the effect of crystal imperfections spoiled the efficiency of channeling while it negligibly affected the performance of volume reflection. We finally propose the usage of the graded crystal as a primary scatterer to aid halo collimation for the new generation of hadronic machines. As a unique feature, a properly cut graded crystal circumvents the problem of the miscut angle, which is currently a severe limitation for implementation of crystal-assisted collimation.

PACS numbers: 61.85.+p, 29.27.−a

Beam manipulation of high- and very-high-energy particle beams is a hot topic in accelerator physics. Coherent effects of ultrarelativistic particles in bent crystals allow steering particle trajectories thanks to the strong electrical field generated between atomic planes and axes [1–3]. Various applications have been proposed and investigated such as beam steering [4], extraction and collimation [5–7] in circular accelerators, as well as splitting and focusing [8] of external beams. Usage of bent crystals for halo collimation of high-energy accelerator has been proposed [9] and demonstrated at Tevatron [10], SPS [11] and U-70 [12] accelerators. Radiation emission due to curved trajectories in bent crystals has been studied to design crystalline undulators [13].

The technique chosen for crystal bending turned out to strongly affect the performance of beam manipulation. Initially, bending methods relied on direct mechanical bending [14], which did not cause a uniform bending of the crystal and required a cm-long crystal along the beam.

Later, a crystal with thickness of few cm along the beam was coated with a ∼10 μm thick film deposited under conditions appropriate to exert a tensile stress on the crystal, resulting in uniform crystal bending [15]. However, in the last ten years new bending methods exploiting secondary parasitic curvature due to anticlastic effect [5] and medium anisotropy (quasimosaic curvatures [16]) were adopted. These techniques allowed bending mm- or sub-mm-thin perfect monocrystals, which performed as record-efficiency deflectors of a high-energy beam through coherent interactions [17,18].

In this Letter we propose the study of a self-standing crystal, i.e., a crystal whose atomic planes are intrinsically and uniformly curved, to manipulate the trajectories of high-energy particles owing to coherent interaction. The method is based on the usage of graded aperiodic $Si_{1-x}Ge_x$ purposely grown with curved atomic planes. A proposal for the application of such a crystal in a new collimation scheme will also be shown.

Ingots of $Si_{1-x}Ge_x$ single crystals were grown by the Czochralski technique [19]. Because of a gradient in Ge concentration, the larger size of Ge atoms with respect to those of Si results in a net curvature of the atomic planes. The lattice parameter of such a crystal changes almost linearly by increasing Ge concentration. $Si_{1-x}Ge_x$ crystals with concentrations up to $x = 7\%$ Ge can be grown with high quality [20,21]. With current fabrication techniques, the curvature radius can be tailored up to some hundreds of meters and down to 15 m. Wafers 500 μm thick were cut from an ingot with the major surfaces of the wafer (111) oriented. Ge concentration was set to produce a cylindrical curvature on a small area [22]. $Si_{1-x}Ge_x$ crystals were introduced in the scientific community to achieve broadband optical components for focusing x and γ rays in a Laue lens [23]. Indeed, the usage of graded $Si_{1-x}Ge_x$ in channeling experiments is not a novelty [24–26]. In those cases, the graded crystal was limited to a film deposited onto a conventional crystalline substrate. In contrast, our crystals have no severe constraint with the thickness, so that bulky graded crystals can easily be produced with a thickness up to some mm. In addition, crystal torsion [27] is prevented for the graded crystal because of the lack of any external bending device, which is needed by a conventional bent crystal.

Striplike crystal was achieved by dicing the wafer on the midplane of the wafer in order to have the crystalline planes perpendicular to the entry face of the beam. If not, a particle with a trajectory parallel to the geometrical main surface of the strip would not be captured under planar channeling at the entry face, but rather it would cross the crystal as if it was an amorphous material or undergo volume reflection [3,17]. Isotropic etching of the crystal was done according to the procedure described in Refs. [28,29] to get rid of the lattice damage induced by the blade while dicing. The strip was characterized with the XPert Pro MRD XL PANalytical^{TM} high-resolution x-ray diffractometer (HR-XRD). A Ge concentration gradient $0.79\% \pm 0.04\%$/cm was deduced by measuring the variation of the lattice interplanar distance of the two faces of the sample [30]. Mosaic-spread measurement by HR-XRD [31] allowed one to determine the curvature radius $R = 25 \pm 3$ m. EPD (etch pit density) of the sample was performed after the experiment. A 10^2 cm^{-2} dislocation density was measured for both the two faces of the strip.

The crystal was mounted on a two-axis goniometric system with angular resolution ~ 1 μrad and tested vs a 400 GeV/c proton beam at the H8 line of the CERN-SPS. The beam was tracked before and after interaction with the crystal by a telescope system of Si strip detectors [32]. Each detector featured ~ 5 μm spatial resolution, resulting in ~ 0.5 μrad angular resolution. The beam size $(1.36 \pm 0.02 \times 0.73 \pm 0.01)$ mm^2 and angular divergence $(10.15 \pm 0.04 \times 8.00 \pm 0.03)$ μrad^2 were measured with the telescope system.

The crystal was aligned with the beam for planar channeling or volume reflection. Under planar channeling, the distribution of the outgoing horizontal deflection angle was fitted with one Gaussian for the channeling peak, one for the undeflected peak and an exponential for the fraction of particles between the two peaks. Under volume reflection, the distribution was fitted with one Gaussian only. Channeling deflection efficiency was computed as the fraction of particles deflected within plus and minus three rms of the Gaussian centered on the mean deflection angle. The efficiency of volume reflection was computed as the fraction of particles deflected within $-\infty$ and plus three rms of the Gaussian. Efficiencies were normalized to the fraction of the particles within plus and minus three rms of the outgoing distribution when the beam impinging on the crystal is misaligned, i.e., when coherent effects do not take place. An exhaustive description of efficiency calculation methodology can be found in Ref. [27]. Torsion measurement was performed by studying the dependence of maximum efficiency peak on the horizontal incoming angle and vertical position.

An analysis was performed over a 500×500 μm^2 portion of the incoming beam centered on the strip. The average channeling deflection angle $\Delta\theta_{x,ch} = 156 \pm 2$ μrad, channeling deflection rms $\sigma_{ch} = 6.6 \pm 0.3$ μrad, and channeling deflection efficiency $\epsilon_{ch} = 62 \pm 3\%$ were measured. Channeling parameters were obtained by selecting a 2 μrad portion of the horizontal divergence of the incoming beam centered on planar channeling alignment, while no selection was applied to vertical divergence. As a result, the crystal bending radius $R = L/\Delta\theta_{x,ch}$ was $R = 25.6 \pm 0.3$ m, $L = 4.00 \pm 0.01$ mm being the crystal length along the beam direction, in good agreement with HR-XRD characterization. The average deflection angle, rms, and deflection efficiency were $\Delta\theta_{x,vr} = -13.5 \pm 0.2$ μrad, $\sigma_{vr} = 7.6 \pm 0.3$ μrad, and $\epsilon_{vr} = 96 \pm 2\%$ for volume reflection (see Fig. 1). Since angular acceptance of volume reflection is equal to the deflection angle of the
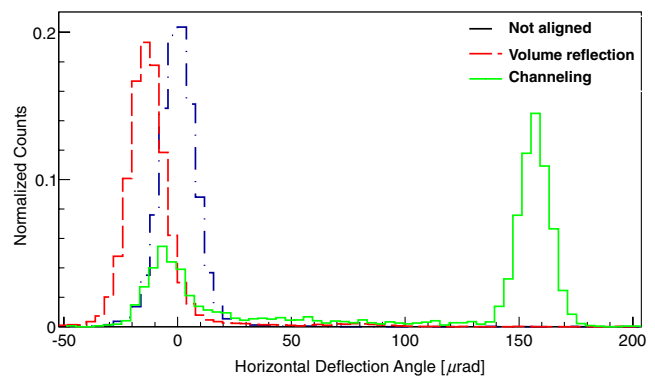

FIG. 1 (color online). Distribution of the deflection angle of particles after the interaction with the crystal aligned for planar channeling (continuous line), for volume reflection (dotted line), and not aligned for any coherent effect (dot-dashed line).

strip [17], no selection was applied to the horizontal and vertical divergences. The torsion was measured to be less than 1 μrad/mm, as expected.

To interpret the experimental data of $Si_{1-x}Ge_x$ crystals, simulation of a strip with the same geometrical features has been worked out through Monte Carlo simulation with the DYNECHARM++ code [33]. A well-established model based on continuum-potential approximation [34,35] was adopted in DYNECHARM++ to integrate the particle trajectory under channeling and volume reflection. The presence of higher atomic-number Ge atoms in the lattice [36] increases the depth of the potential well [see Fig. 2(a)], slightly affecting the channeling critical angle ($\simeq 9.6$ μrad vs $\simeq 9.5$ μrad) with respect to pure Si crystal. Thereby, the average contribution of Ge atoms has been included in the calculation of the continuous potential averaged along main planes [37,38]. The enhancement of static lattice disorder caused by the coexistence of different bond lengths in the crystalline matrix negligibly alters the efficiency because the maximum difference between the Ge-Si and Si-Si bond length is $\sim$0.02 Å for diluted Ge concentration [36]. Therefore, atomic static displacement cannot exceed this value, causing a small increase in the Debye-Waller factor and a consequent decrease in channeling deflection efficiency to less than 1% [39].

Because of the non-negligible number of defects in the crystal, the contribution of defects was also taken into consideration. Various kinds of defects may affect the
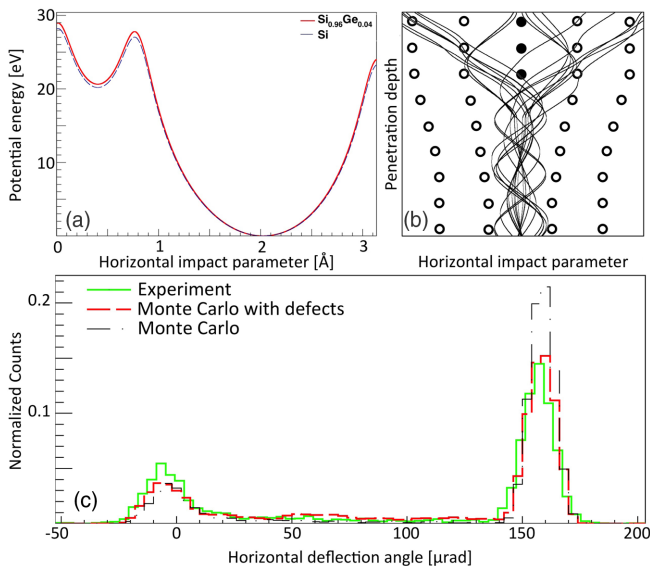

FIG. 2 (color online).   (a) Average (111) interplanar potential energy for a perfect Si crystal and for a $Si_{0.96}Ge_{0.04}$ crystal. (b) Qualitative schemes of lattice misalignment due to edge dislocation and its influence on particle trajectories. (c) Experimental data (continuous line), Monte Carlo simulation (dot-dashed line) and Monte Carlo simulation including the presence of defects (dotted line) of the distribution of horizontal deflection angles of particles after the interaction with the crystal aligned for planar channeling.

displacement of the atoms in a crystal. Defects can be grouped by the number of dimensions in the lattice on which they act, i.e., pointlike (interstitial atoms and vacancies), linear (dislocations), two-dimensional (stacking-faults), and three-dimensional (amorphous clusters) defects [40]. Defects are typically described through the Burger vector, i.e., a vector that represents the magnitude and direction of the lattice distortion of defects in the crystal [41].

According to a specific investigation about the influence of defects on the channeling of high-energy particles [42], pointlike and third-order defects negligibly affect channeling efficiency ($\ll 0.01\%$). On the contrary, the presence of a single stacking fault would cause too strong a reduction ($\simeq 65\%$) of the channeling efficiency with respect to experimental results. Therefore they are not to be considered in our case. On the other hand, since the first-order defect would affect the channeling efficiency by approximately the same order of magnitude as the values experimentally observed, this kind of defect must be thoroughly considered for simulating the particle dynamics in the crystal. As depicted in Fig. 2(b), the first-order dislocation manifests itself as an extra-plane which causes a stress field around the edge.

The ECHARM_DEFECT C++ class has been specifically developed for the DYNECHARM++ toolkit to simulate the influence of defects on the coherent effect. The displacement field for the edge defect is quantified through experimentally verified [43] analytical equations [44]. Starting by the displacement field, its derivatives and particle position and momentum vectors, the point-to-point centrifugal force acting on the particle is computed in the reference frame orthogonal to the crystal planes. The position of each dislocation is randomly generated by defining the number of dislocation per cm^2.

Monte Carlo simulations with and without the presence of edge dislocations have been performed to quantify their influence on coherent effects. Measured beam parameters and the dislocation density per cm^2 have been used as inputs. Electrical characteristics of the $Si_{1-x}Ge_x$ have been evaluated by considering the influence of both Si and Ge atoms. Calculated efficiency for channeling and volume reflection are $\epsilon_{ch,MC} = 76.5 \pm 1.5\%$ and $\epsilon_{vr,MC} = 98.0 \pm 0.5\%$, respectively. Once the dislocations are included, the same physical quantities hold $\epsilon_{ch,MC,dis} = 62.5 \pm 1.5\%$ and $\epsilon_{vr,MC,dis} = 96.5 \pm 1.0\%$. Figure 2(c) shows a comparison between the experimental record and the Monte Carlo simulations.

As expected, the probability to undergo dechanneling, i.e., to leave the channeling state, rises up because of the presence of the strain field generated by defects. Such an effect manifests itself all the way along the trajectory [see Fig. 2(b)] of a channeled particle in the crystal and consequently spoils deflection efficiency. On the contrary, volume reflection acts within one particle oscillation in the crystal, i.e., for about a few tens of μm at 400 GeV/c. Hence, the presence of neither Ge atoms nor defects are

crucial and deflection efficiency is very much the same as for a perfect bent crystal. In some more general sense, volume reflection is more robust than channeling vs the presence of crystal imperfection and/or impurities, and that explains why the latter has been observed to perform very efficiently with high-energy particles solely in the cases of Si [18] and high-purity Ge [45].

Although $Si_{1-x}Ge_x$ crystals have not proved to perform vs channeling so efficiently as single Si and Ge monocrystals, we propose to use such crystals as a hybrid solution for the collimation of high-energy particle beams as explained herewith.

The problem of beam collimation is a mandatory task for the currently operational Large Hadron Collider (LHC) because of the need for cleaning halo particles. Indeed, their stray trajectories would hit the superconducting magnets, provoking quenching and ultimately their damage. Currently operating primary collimators act as scatterers [46–48], whose diffused particles are captured in cascade by the secondary and the tertiary collimators. Primary collimators are 20 cm long and made of amorphous graphite. Their flatness must be no greater than 25 μm and roughness less than 1 μm [48,49]. As an alternative, the usage of short bent crystals has been proposed to aid in the collimation of the intense beam halo in the LHC [50–52]. Bent crystals capture beam particles under the planar-channeling regime and the particles follow the crystal curvature; i.e., the beam is being steered by the bent atomic planes. On the strength of recent optimization in the manufacture techniques of the crystals [28,29] and their bending devices [53], the UA9 collaboration is pursuing the goal of crystal-assisted collimation with a campaign of experiments, which has demonstrated the validity of this scheme for operation with protons [11,54] and even for ions [55]. Crystal collimation takes advantage of the consistent reduction of nuclear interactions for both protons and ions [56]. These two schemes and the corresponding dynamics of particles are illustrated in Figs. 3(a) and 3(b).

As depicted in Fig. 3(c), a $Si_{1-x}Ge_x$ graded crystal encompasses, in a single device, flat morphology, which is an advantage of amorphous scatterers, and coherent effects, which is an advantage of crystals. In fact, these apparently antithetical conditions are fully met in such a crystal whose atomic planes are curved surfaces. As a result, graded crystals can fruitfully serve for collimation, not for their particularly high deflection performance, which is lower than for a Si crystal, but rather for the usefulness given by their specific characteristics.

In fact, a $Si_{1-x}Ge_x$ graded crystal can be used to upgrade existing collimation systems. Properly sized crystals could be accommodated to cover the surfaces exposed to the beam of existing primary amorphous collimators. In this way, collimation via coherent effects in crystals could be done, without changing already installed moving and control systems. Furthermore, volume reflection in $Si_{1-x}Ge_x$ exhibits
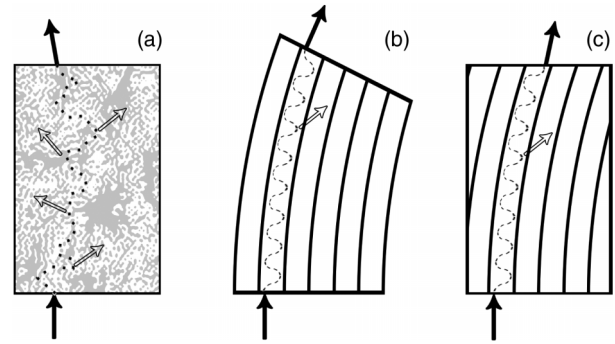

FIG. 3. Schemes of interaction of a particle with (a) amorphous scatterer, (b) mechanically bent monocrystal, (c) self-bent monocrystal. The proportions of the crystal dimensions are not in scale. Filled black arrows are the incoming and outgoing directions of a particle interacting with the collimator, dotted lines are the trajectories of the particles inside the amorphous collimator, dashed lines are trajectories of the particles inside the crystal and the hybrid collimators, white arrows with black borders are secondary particles generated in the interaction with the primary collimator.

the same efficiency and acceptance as for a perfect Si crystal and such a scheme has been proved to work in collimation experiments [11,54,55]. All the needed surface parameters can satisfactorily be met with standard semiconductor techniques. In addition, $Si_{1-x}Ge_x$ crystals can be used as tiles in a large-area bent crystal shield for deflection of high energy ions as suggested in Ref. [57].

According to experiments [54,58,59] and recent studies [60], the most crucial parameter affecting the performance of crystals as collimator is the miscut angle, namely the angle between the morphological surface of the crystal and the crystalline channeling planes. A miscut features a positive [Fig. 4(a)] or negative [Fig. 4(c)] angle with
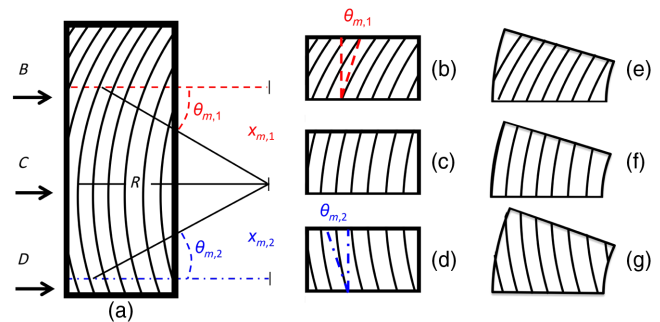

FIG. 4 (color online). Schemes of the correlation between a miscut angle and the cut position. The proportions of the crystal dimensions are not in scale. (a) Initial wafer and three cut positions (B, C, D). (b) Graded crystal with positive miscut angle $\theta_{m,1} \simeq x_{m,1}/R$ obtained by cutting the wafer at point B. (c) Graded crystal with zero miscut angle [as that in Fig. 3(c)] obtained by cutting the wafer at point C. (d) Graded crystal with negative miscut angle $\theta_{m,2} \simeq x_{m,2}/R$ obtained by cutting the wafer at point D. (e), (f) and (g) are three conventional bent crystals with the same miscut angle as in (a), (b), and (c), respectively.

respect to the planes. The latter is very undesirable, because channeled particles can exit the crystal without passing the full length and therefore experience a smaller bending angle. According to recent studies [60], it was suggested to fabricate a crystal with a miscut angle less than 10 μrad to mitigate the effect of a miscut for collimation in the LHC. Here we demonstrate that a graded crystal could be a tool to circumvent the problem of a miscut, because a graded crystal is equivalent to a bent crystal with the same curvature radius and arbitrarily chosen miscut angle. In fact, a $Si_{1-x}Ge_x$ strip can be diced off by a Si-Ge wafer orthogonal to the crystalline planes with sub-μrad angular precision through the usage of commercial diamond-blade dicing machines. As shown in Fig. 4, misplacements $x_{m,1}$ and $x_{m,2}$ of the dicing point from the point orthogonal to crystal planes give rise up to miscut angles $\theta_{m,1} = x_{m,1}/R$ and $\theta_{m,1} = x_{m,1}/R$ μrad. Owing to μm precision in the cut orthogonal to the strip surface and ~ 10 μm precision in the determination of the position to be cut through x-ray diffractometry, as low a miscut as 10 μrad can be actually reached for a graded crystal with $R = 25$ m. For a larger radius as that foreseen for the LHC, such precision becomes still better.

In summary, the dynamics of high-energy particles under channeling and volume reflection have been studied for a graded bulky $Si_{1-x}Ge_x$ crystal through experimental work. The intrinsically curved crystalline planes made the crystal a reliable device for manipulation of the trajectories of high-energy particles via either channeling or volume reflection. A Monte Carlo simulation has been worked out to highlight the influence of Ge atoms and lattice defects under planar channeling in a $Si_{1-x}Ge_x$ crystal. A novel collimation scheme based on a hybrid design between standard and crystal-assisted collimation has been proposed as a possible upgrade of existing collimation systems used in high-energy particle accelerators. This scheme circumvents the critical problem of the miscut angle for crystal-assisted collimation, which is currently the most severe limitation for its application in high-energy accelerators, especially to the LHC.

---

*Corresponding author.
guidi@fe.infn.it

[1] E. Tsyganov, Fermilab Tech. Report No. TM-682, 1976.
[2] E. Tsyganov, Fermilab Tech. Report No. TM-684, 1976.
[3] A. Taratin and S. Vorobiev, Phys. Lett. A **119**, 425 (1987).
[4] A. F. Elishev et al., Phys. Lett. **88B**, 387 (1979).
[5] A. G. Afonin et al., Phys. Rev. Lett. **87**, 094802 (2001).
[6] R. A. Carrigan et al., Phys. Rev. ST Accel. Beams **5**, 043501 (2002).
[7] R. P. Fliller, A. Drees, D. Gassner, L. Hammons, G. McIntyre, S. Peggs, D. Trbojevic, V. Biryukov, Y. Chesnokov, and V. Terekhov, Nucl. Instrum. Methods Phys. Res., Sect. B **234**, 47 (2005).
[8] A. S. Denisov et al., Nucl. Instrum. Methods Phys. Res., Sect. B **69**, 382 (1992).
[9] M. Maslov, N. Mokhov, and I. Yazynin, SSCL Tech. Report No. SSCL 484, 1991.
[10] V. D. Shiltsev et al., Proceedings of 1st International Particle Accelerator Conference (IPAC'10), Kyoto, Japan, 2010, econf C100523, TUOAMH03 (2010).
[11] W. Scandale et al., Phys. Lett. B **692**, 78 (2010).
[12] A. G. Afonin et al., Instrum. Exp. Tech. **54**, 1 (2011).
[13] A. V. Korol, A. V. Solov'yov, and W. Greiner, Int. J. Mod. Phys. E **13**, 867 (2004).
[14] S. I. Baker et al., Phys. Lett. **137B**, 129 (1984).
[15] J. S. Forster et al., Nucl. Phys. **B318**, 301 (1989).
[16] Y. Ivanov, A. Petrunin, and V. Skorobogatov, J. Exp. Theor. Phys. Lett. **81**, 99 (2005).
[17] W. Scandale et al., Phys. Rev. Lett. **98**, 154801 (2007).
[18] W. Scandale et al., Phys. Lett. B **680**, 129 (2009).
[19] J. Czochralski, Z. Phys. Chem., Abt. A **92**, 219 (1918).
[20] N. V. Abrosimov, S. N. Rossolenko, V. Alex, A. Gerhardt, and W. Schröder, J. Cryst. Growth **166**, 657 (1996).
[21] N. V. Abrosimov, S. N. Rossolenko, W. Thieme, A. Gerhardt, and W. Schröder, J. Cryst. Growth **174**, 182 (1997).
[22] R. Smither, K. Abu Saleem, M. Beno, C. Kurtz, A. Khounsary, and N. Abrosimov, Rev. Sci. Instrum. **76**, 123107 (2005).
[23] N. V. Abrosimov, Exp. Astron. **20**, 185 (2005).
[24] D. G. de Kerckhove, M. B. H. Breese, P. J. M. Smulders, and D. N. Jamieson, Appl. Phys. Lett. **74**, 227 (1999).
[25] M. B. H. Breese, D. G. de Kerckhove, P. J. M. Smulders, W. M. Arnold Bik, and D. O. Boerma, Nucl. Instrum. Methods Phys. Res., Sect. B **171**, 387 (2000).
[26] H. L. Seng, M. B. H. Breese, F. Watt, M. Kummer, and H. von Känel, Nucl. Instrum. Methods Phys. Res., Sect. B **215**, 235 (2004).
[27] W. Scandale et al., Phys. Rev. ST Accel. Beams **11**, 063501 (2008).
[28] S. Baricordi, V. Guidi, A. Mazzolari, D. Vincenzi, and M. Ferroni, J. Phys. D **41**, 245501 (2008).
[29] S. Baricordi et al., Applied Phys. Lett. **91**, 061908 (2007).
[30] J. P. Dismukes, L. Ekstrom, and R. J. Paff, J. Phys. Chem. **68**, 3021 (1964).
[31] V. Guidi, A. Mazzolari, D. De Salvador, and A. Carnera, J. Phys. D **42**, 182005 (2009).
[32] L. Celano, D. Creanza, M. de Palma, G. Maggi, L. Fiore, V. Paticchio, G. Raso, G. Selvaggi, L. Silvestris, and P. Tempesta, Nucl. Instrum. Methods Phys. Res., Sect. A **381**, 49 (1996).
[33] E. Bagli and V. Guidi, Nucl. Instrum. Methods Phys. Res., Sect. B, doi: 10.1016/j.nimb.2013.01.073 (2013).
[34] J. Lindhard, K. Dan. Vidensk. Selsk. Mat. Fys. Medd. **34**, 14 (1965).
[35] A. Taratin, Phys. Part. Nucl. **29**, 437 (1998).
[36] J. C. Aubry, T. Tyliszczak, A. P. Hitchcock, J. M. Baribeau, and T. E. Jackman, Phys. Rev. B **59**, 12872 (1999).

[37] E. Bagli, V. Guidi, and V. A. Maisheev, Phys. Rev. E **81,** 026708 (2010).

[38] E. Bagli, V. Guidi, and V. A. Maisheev, *Proceedings of 1st International Particle Accelerator Conference (IPAC'10), Kyoto, Japan, 2010,* econf C100523, TUPEA070 (2010).

[39] V. M. Biryukov, Y. A. Chesnekov, and V. I. Kotov, *Crystal Channeling and Its Applications at High-Energy Accelerators* (Springer, New York, 1996).

[40] L. Feldman, J. Mayer, and S. Picraux, *Materials Analysis by Ion Channeling* (Academic, New York, 1982).

[41] C. Kittel, *Introduction to Solid State Physics* (John Wiley & Sons, New York, 1996), 7th ed.

[42] V. M. Biryukov, Phys. Rev. E **52,** 2045 (1995).

[43] M. J. Hytch, J.-L. Putaux, and J.-M. Penisson, Nature (London) **423,** 270 (2003).

[44] J. P. Hirth and J. Lothe, *Theory of Dislocations* (Wiley, New York, 1982), 2nd ed, Vol. 1.

[45] D. De Salvador *et al.,* Appl. Phys. Lett. **98,** 234102 (2011).

[46] S. Redaelli, R. Assmann, A. Masi, and R. Losito, *Proceedings of the 23rd Particle Accelerator Conference (PAC'09), Vancouver, BC, Canada, 2009* (Triumf, Vancouver, 2010), pp. FR5REP007.

[47] R. Assmann, *Proceedings of the 23rd Particle Accelerator Conference (PAC'09), Vancouver, BC, Canada, 2009* (Triumf, Vancouver, 2010), pp. TU4GRI01.

[48] O. S. Brning *et al.,* *LHC Design Report* (CERN, Geneva, 2004).

[49] R. Assmann *et al., Proceedings of 8th European Particle Accelerator Conference (EPAC'02), Paris, France, 2002* (CERN, Geneva, 2002), p. 64.

[50] V. M. Biryukov, V. N. Chepegin, Y. A. Chesnokov, V. Guidi, and W. Scandale, Nucl. Instrum. Methods Phys. Res., Sect. B **234,** 23 (2005).

[51] R. Assmann, S. Redaelli, and W. Scandale, *Proceedings of 10th European Particle Accelerator Conference (EPAC'06), Edinburgh, Scotland, 2006,* edited by C. Prior (CERN, Geneva, 2006), pp. TUPLS017.

[52] W. Scandale *et al.,* CERN Report No. CERN-LHCC-2011-007/LHCC-I-019, 2011.

[53] A. Mazzolari *et al., Proceedings of 1st International Particle Accelerator Conference (IPAC'10), Kyoto, Japan, 2010,* econf C100523, TUPEC080 (2010).

[54] W. Scandale *et al.,* Phys. Lett. B **703,** 547 (2011).

[55] W. Scandale *et al.,* Phys. Lett. B **714,** 231 (2012).

[56] W. Scandale *et al.,* Nucl. Instrum. Methods Phys. Res., Sect. B **268,** 2655 (2010).

[57] M. B. H. Breese, Appl. Phys. Lett. **91,** 261901 (2007).

[58] K. Elsener, G. Fidecaro, M. Gyr, W. Herr, J. Klem, U. Mikkelsen, S. P. Møller, E. Uggerhøj, G. Vuagnin, and E. Weisse, Nucl. Instrum. Methods Phys. Res., Sect. B **119,** 215 (1996).

[59] N. Mokhov, G. Annala, and A. Apyan, *Proceedings of the 23rd Particle Accelerator Conference (PAC'09), Vancouver, BC, Canada, 2009* (Triumf, Vancouver, 2010), pp. WE1GRC05.

[60] V. Tikhomirov and A. Sytov, Prob. Atomic Sci. Technol. **57,** 88 (2012).